JHEP

Published for SISSA by Springer

Received: April 13, 2016
Revised: January 21, 2017
Accepted: March 29, 2017
Published: April 7, 2017

# Majorana dark matter with B+L gauge symmetry

**Wei Chao,**[a,b] **Huai-Ke Guo**[a] **and Yongchao Zhang**[c]

[a] *Amherst Center for Fundamental Interactions, Department of Physics, University of Massachusetts-Amherst, Amherst, MA 01003 United States*

[b] *Center for Advanced Quantum Studies, Department of Physics, Beijing Normal University, Beijing, 100875, China*

[c] *Service de Physique Théorique, Université Libre de Bruxelles, Boulevard du Triomphe, CP225, 1050 Brussels, Belgium*

*E-mail:* chao@physics.umass.edu, huaike@physics.umass.edu, yongchao.zhang@ulb.ac.be

Abstract: We present a new model that extends the Standard Model (SM) with the local $\mathbf{B}+\mathbf{L}$ symmetry, and point out that the lightest new fermion $\zeta$, introduced to cancel anomalies and stabilized automatically by the $\mathbf{B}+\mathbf{L}$ symmetry, can serve as the cold dark matter candidate. We study constraints on the model from Higgs measurements, electroweak precision measurements as well as the relic density and direct detections of the dark matter. Numerical results reveal that the pseudo-vector coupling of $\zeta$ with $Z$ and the Yukawa coupling with the SM Higgs are highly constrained by the latest results of LUX, while there are viable parameter space that could satisfy all the constraints and give testable predictions.

Keywords: Beyond Standard Model, Cosmology of Theories beyond the SM, Gauge Symmetry

ArXiv ePrint: 1604.01771



doi:10.1007/JHEP04(2017)034

JHEP04(2017)034

## Contents



## 1 Introduction

The Standard Model (SM) of particle physics is in spectacular agreement with almost all experiments, but there are still observations that are not accessible solely by the SM. Accumulating evidences point to the existence of dark matter, which is neutral, colorless, stable and weakly interacting particle that accounts for about 26.8% [1] of the matter in the Universe. We know little about the nature of dark matter i.e. its mass, spin and stability as well as how it interacts with the SM particles. To accommodate the dark matter, SM has to be extended with new particle and new symmetry.

The baryon number (**B**) and the lepton number (**L**) are accidental global symmetries in the SM. **B** must be violated to explain the baryon asymmetry of the Universe. **L** will be violated if active neutrinos are Majorana particles, which may be tested in neutrinoless double beta decay experiments. It was shown that **B** and **L** [2–6] as well as $\mathbf{B}-\mathbf{L}$ [7] can be local gauge symmetries. The case of $\mathbf{B}+\mathbf{L}$ as a local gauge symmetry was originally pointed out in refs. [8, 9], but its phenomenology was not studied in detail. In this paper we investigate the $\mathbf{B}+\mathbf{L}$ symmetry based on the *dark matter* motivation. As will be shown in this paper, the lightest extra fermion, introduced to cancel anomalies, is automatically stabilized by the $\mathbf{B}+\mathbf{L}$ symmetry and can naturally serve as the cold dark matter candidate. This scenario is interesting and economical since one does not need to introduce extra symmetry to stabilize the dark matter. We study constraints on the model from Higgs measurements and electroweak precision measurements, and then focus on the phenomenology of the Majorana dark matter. We search for the parameter space that may accommodate both the observed dark matter relic density and constraints of direct detections. Our results show that

- The $Z'$ gauge boson mainly contributes to the annihilation of the dark matter $\zeta$, and the $\zeta\zeta \to Z' \to Vh(s)$ process dominates the annihilation of heavy $\zeta$. Its contribution to the direct detection cross section is suppressed by the velocity of the dark matter.



JHEP04(2017)034

| SM particles | $G_{\rm SM}$ | $\mathrm{U}(1)_{\rm B+L}$ | BSM particles | $G_{\rm SM}$ | $\mathrm{U}(1)_{\rm B+L}$ |
|---|---|---|---|---|---|
| $q_L$ | $(3,\ 2,\ 1/6)$ | $\frac{1}{3}$ | $\psi_L$ | $(1,\ 2,\ -1/2)$ | -3 |
| $u_R$ | $(3,\ 1,\ 2/3)$ | $\frac{1}{3}$ | $\psi_R$ | $(1,\ 2,\ -1/2)$ | 3 |
| $d_R$ | $(3,\ 1,\ -1/3)$ | $\frac{1}{3}$ | $\chi_R$ | $(1,\ 1,\ 0)$ | -3 |
| $\ell_L$ | $(1,\ 2,\ -1/2)$ | 1 | $E_R$ | $(1,\ 1,\ -1)$ | -3 |
| $e_R$ | $(1,\ 1,\ -1)$ | 1 | $\chi_L$ | $(1,\ 1,\ 0)$ | 3 |
| $\nu_R$ | $(1,\ 1,\ 0)$ | 1 | $E_L$ | $(1,\ 1,\ -1)$ | 3 |
| $H$ | $(1,\ 2,\ 1/2)$ | 0 | $S$ | $(1,\ 1,\ 0)$ | 6 |

**Table 1**. Quantum numbers of fields under the gauge symmetries $G_{\rm SM}\times \mathrm{U}(1)_{\rm B+L}$, where $G_{\rm SM} = \mathrm{SU}(3)_C\times \mathrm{SU}(2)_L\times \mathrm{U}(1)_Y$.

- The pseudo-vector coupling $\zeta$ with $Z$ is suppressed by the latest PandaX-II result on the spin-dependent cross section, and the upper limit on this coupling is about 0.037.
- Yukawa couplings of $\zeta\bar{\zeta}$ with Higgs are suppressed by the latest LUX 2016 result on spin-independent direct detection cross section, while there are adequate parameter space that may satisfy all constraints.

It should be mentioned that the $\mathbf{B}+\mathbf{L}$ is a brand-new symmetry that deserves further detailed study in many aspects, such as the collider signature, neutrino masses, baryon asymmetry and sphaleron etc, which, interesting but beyond the reach of this paper, will be shown in the follow-up paper.

The remaining of the paper is organized as follows: in section 2 we briefly describe our model. We study constraints of Higgs measurements and oblique parameters in section 3. Section 4 is devoted to the study of the dark matter phenomenology. In section 5 we study collider signatures of the dark matter. The last part is the concluding remarks.

## 2 The model

When the SM is extended by the local $\mathbf{B}+\mathbf{L}$ symmetry, anomalies are not automatically cancelled as in the minimal SM. One simple way out is to introduce, in addition to the right-handed neutrinos, extra vector-like fermions at the TeV scale so as to cancel various anomalies. To break the $\mathrm{U}(1)_{\rm B+L}$ gauge symmetry via the Higgs mechanism, we introduce a singlet scalar $S$ with $\mathrm{B}+\mathrm{L}$ charge of $-6$. All the particle contents and their quantum numbers under the gauge group $G_{\rm SM}\times \mathrm{U}(1)_{\rm B+L}\equiv \mathrm{SU}(3)_C\times \mathrm{SU}(2)_L\times \mathrm{U}(1)_Y\times \mathrm{U}(1)_{\rm B+L}$ are listed in table 1. It is easy to check that all potential anomalies are canceled in this simple framework, i.e. $\mathcal{A}_1(\mathrm{SU}(3)_C^2\otimes \mathrm{U}(1)_{\rm B+L})$, $\mathcal{A}_2(\mathrm{SU}(2)_L^2\otimes \mathrm{U}(1)_{\rm B+L})$, $\mathcal{A}_3(\mathrm{U}(1)_Y^2\otimes \mathrm{U}(1)_{\rm B+L})$, $\mathcal{A}_4(\mathrm{U}(1)_Y\otimes \mathrm{U}(1)_{\rm B+L}^2)$, $\mathcal{A}_5(\mathrm{U}(1)_{\rm B+L}^3)$ and $\mathcal{A}_6(\mathrm{U}(1)_{\rm B+L})$. We refer the reader to refs. [8, 9] for the details of anomaly cancellation.

The most general Higgs potential takes the following form:

$$V = -\mu_h^2 H^\dagger H + \lambda_h (H^\dagger H)^2 - \mu_s^2 S^\dagger S + \lambda_s (S^\dagger S)^2 + \lambda_{sh} S^\dagger S H^\dagger H\ , \tag{2.1}$$

where $H\equiv (G^+, \rho_h + iG^0 + v_h/\sqrt{2})^T$ is the SM Higgs with $v_h$ its vacuum expectation value (VEV), and $S\equiv (\rho_s + iG_s^0 + v_s)/\sqrt{2}$ with $v_s$ the VEV of $S$. After imposing the



JHEP04(2017)034

| $s_i s_j s_k$ | $C_{s_i s_j s_k}$ |
|---|---|
| $h^3$ | $3m_h^2\left(\frac{c_\theta^3}{v}+\frac{s_\theta^3}{v_s}\right)$ |
| $s^3$ | $3m_s^2\left(\frac{c_\theta^3}{v_s}-\frac{s_\theta^3}{v}\right)$ |
| $h^2 s$ | $s_\theta c_\theta\left(2m_h^2+m_s^2\right)\left(\frac{s_\theta}{v_s}-\frac{c_\theta}{v}\right)$ |
| $hs^2$ | $s_\theta c_\theta\left(m_h^2+2m_s^2\right)\left(\frac{s_\theta}{v}+\frac{c_\theta}{v_s}\right)$ |

**Table 2**. Trilinear couplings. Feynman rules are obtained by adding the multiplication factor $(-i)$.

minimization conditions, one has $\mu_h^2 = \lambda_h v_h^2 + \frac{\lambda_{sh} v_s^2}{2}$ and $\mu_s^2 = \lambda_s v_s^2 + \frac{\lambda_{sh} v_h^2}{2}$. Due to the last term in eq. (2.1), $\rho_s$ is mixed with $\rho_h$ to form mass eigenstates $s, h$, and the relations between mass eigenstates and interaction eigenstates take the following form,

$$\begin{aligned} s &= c_\theta \rho_s - s_\theta \rho_h, \\ h &= s_\theta \rho_s + c_\theta \rho_h, \end{aligned} \tag{2.2}$$

where $c_\theta = \cos\theta$ and $s_\theta = \sin\theta$, with $\theta$ the mixing angle that diagonalizes the CP-even scalar mass matrix. The parameters $\lambda_s$, $\lambda_h$ and $\lambda_{sh}$ in the potential can be reconstructed by the physical parameters $m_s$, $m_h$, $\theta$, $v_h$ and $v_s$ as:

$$\lambda_h = \frac{m_h^2 c_\theta^2 + m_s^2 s_\theta^2}{2{v_h}^2}, \qquad \lambda_s = \frac{m_h^2 s_\theta^2 + m_s^2 c_\theta^2}{2v_s^2}, \qquad \lambda_{sh} = \frac{(m_h^2 - m_s^2) s_\theta c_\theta}{v_h v_s}. \tag{2.3}$$

Trilinear scalar interactions are listed in table. 2. After the spontaneous breaking of the $\mathrm{U}(1)_{\mathrm{B+L}}$, the $Z'$ bosons obtain its mass:

$$M_{Z'} = 6 g_{\mathrm{B+L}} v_s \ , \tag{2.4}$$

where $g_{\mathrm{B+L}}$ is the gauge coupling of $\mathrm{U}(1)_{\mathrm{B+L}}$.

Due to their special $\mathbf{B+L}$ charge new fermions do not couple directly to the SM fermion. New Yukawa interactions can be written as

$$\begin{aligned} -\mathcal{L} \supset\ & y_8 \overline{\psi}_L S^* \psi_R + y_2 \overline{\chi_L} S \chi_R + \frac{1}{2} y_5 \overline{\chi_R^C} S \chi_R + \frac{1}{2} y_1 \overline{\chi_L} S \chi_L^C + y_6 \overline{\psi_L} \tilde{H} \chi_R \\ & + y_3 \overline{\psi_L} \tilde{H} \chi_L^C + y_4 \overline{\chi_L} \psi_R^T \varepsilon H + y_7 \overline{\chi_R^C} \psi_R^T \varepsilon H + \mathrm{h.c}, \end{aligned} \tag{2.5}$$

where $\psi_{L,R} \equiv (N,\ \Sigma)_{L,R}^T$ and we have neglected Yukawa interactions of charged fermions. One might write down the mass matrix $(\mathcal{M})$ of neutral fermions in the basis of $\xi \equiv (\chi_L,\ \chi_R^C,\ N_L,\ N_R^C)^T$:

$$\frac{1}{2\sqrt{2}} \overline{\begin{pmatrix} \chi_L & \chi_R^C & N_L & N_R^C \end{pmatrix}} \begin{pmatrix} y_1 v_s & y_2 v_s & y_3 v_h & y_4 v_h \\ \bigstar & y_5 v_s & y_6 v_h & y_7 v_h \\ \bigstar & \bigstar & 0 & y_8 v_s \\ \bigstar & \bigstar & \bigstar & 0 \end{pmatrix} \begin{pmatrix} \chi_L^C \\ \chi_R \\ N_L^C \\ N_R \end{pmatrix} + \mathrm{h.c.} \tag{2.6}$$

where the mass matrix is symmetric. $\mathcal{M}$ can be diagonalized by a $4\times4$ unitary transformation: $\mathcal{U}^\dagger \mathcal{M} U^* = \widehat{\mathcal{M}}$, where $\widehat{\mathcal{M}} = \mathrm{diag}\{m_1,\ m_2,\ m_3,\ m_4\}$. Yukawa couplings in eq. (2.6) can then be reconstructed by the mass eigenvalues and mixing angles, which are collected



JHEP04(2017)034

| | | | |
|---|---|---|---|
| $y_1$ | $\sqrt{2}v_s^{-1}\sum_i^4 m_i\mathcal{U}_{1i}^2$ | $y_5$ | $\sqrt{2}v_s^{-1}\sum_i^4 m_i\mathcal{U}_{2i}^2$ |
| $y_2$ | $\sqrt{2}v_s^{-1}\sum_i^4 m_i\mathcal{U}_{1i}\mathcal{U}_{2i}$ | $y_6$ | $\sqrt{2}v_h^{-1}\sum_i^4 m_i\mathcal{U}_{2i}\mathcal{U}_{3i}$ |
| $y_3$ | $\sqrt{2}v_h^{-1}\sum_i^4 m_i\mathcal{U}_{1i}\mathcal{U}_{3i}$ | $y_7$ | $\sqrt{2}v_h^{-1}\sum_i^4 m_i\mathcal{U}_{2i}\mathcal{U}_{4i}$ |
| $y_4$ | $\sqrt{2}v_h^{-1}\sum_i^4 m_i\mathcal{U}_{1i}\mathcal{U}_{4i}$ | $y_8$ | $\sqrt{2}v_s^{-1}\sum_i^4 m_i\mathcal{U}_{3i}\mathcal{U}_{4i}$ |

**Table 3**. Yukawa couplings in term of physical parameters.

in table 3. In this case the relation between interaction eigenstates and mass eigenstates can be written as

$$\xi_i = \sum_j \mathcal{U}_{ij}\hat{\xi}_j \,. \tag{2.7}$$

We identify the fermion $\hat{\xi}_1$ as the cold dark matter candidate and define the Majorana field as $\zeta \equiv \hat{\xi}_1 + \hat{\xi}_1^C$. Interactions of $\zeta$ with the mediators $Z'$, $Z$, $\rho_s$ and $\rho_h$ can be written as

$$\begin{array}{ll}
\mathcal{C}_1\overline{\zeta}\rho_s\zeta & : \mathcal{C}_1 = \frac{1}{\sqrt{2}}\left(\frac{1}{2}y_1\mathcal{U}_{11}^2 + \frac{1}{2}y_5\mathcal{U}_{21}^2 + y_2\mathcal{U}_{11}\mathcal{U}_{21} + y_8\mathcal{U}_{31}\mathcal{U}_{41}\right) \\
\mathcal{C}_2\overline{\zeta}\rho_h\zeta & : \mathcal{C}_2 = \frac{1}{\sqrt{2}}\left(y_6\mathcal{U}_{31}\mathcal{U}_{21} + y_7\mathcal{U}_{21}\mathcal{U}_{41} + y_3\mathcal{U}_{31}\mathcal{U}_{11} + y_4\mathcal{U}_{11}\mathcal{U}_{41}\right) \\
\mathcal{C}_3\overline{\zeta}\gamma_\mu\gamma_5\zeta Z'^\mu & : \mathcal{C}_3 = \frac{3}{2}g_{\mathrm{B+L}}\left(\mathcal{U}_{11}^2 + \mathcal{U}_{21}^2 - \mathcal{U}_{31}^2 - \mathcal{U}_{41}^2\right) \\
\mathcal{C}_4\overline{\zeta}\gamma_\mu\gamma_5\zeta Z^\mu & : \mathcal{C}_4 = \frac{g}{4c_W}\left(\mathcal{U}_{41}^2 - \mathcal{U}_{31}^2\right)
\end{array} \tag{2.8}$$

where $\rho_s$ and $\rho_h$ are given in interaction eigenstates. When studying the phenomenology of the dark matter, e.g. the relic abundance and direct detection, they need to be rotated to the mass eigenstates and the corresponding couplings (for $s$ and $h$ respectively) turn to:

$$\begin{aligned}
\widehat{\mathcal{C}}_1 &= \cos\theta\mathcal{C}_1 - \sin\theta\mathcal{C}_2 \,, \\
\widehat{\mathcal{C}}_2 &= \cos\theta\mathcal{C}_2 + \sin\theta\mathcal{C}_1 \,.
\end{aligned} \tag{2.9}$$

It should be mentioned that the technique of cancelling anomalies of $\mathbf{B}$ and(or) $\mathbf{L}$ with new vector-like fermions was proposed in refs. [3, 4]. Here we apply it to eliminate anomalies of the local $\mathbf{B}+\mathbf{L}$ in this paper. To distinguish our case from those proposed in refs. [2–6], one needs to precisely detect the decay channels and rates of $Z'$, where for our case, the rate of $Z'$ to SM leptons is about three times as large as the rate of $Z'$ to SM quarks. To distinguish the local $\mathbf{B}+\mathbf{L}$ from the conventional local $\mathbf{B}-\mathbf{L}$, one may detect couplings of new charged fermions with $Z'$. For the conventional $\mathbf{B}-\mathbf{L}$, there is no such couplings. One may also check the running behavior of the new U(1) gauge coupling. As will be shown in the next section, the $\beta$-function of $g_{\mathbf{B+L}}$ is very different from that of $g_{\mathbf{B-L}}$.

## 3 Constraints

Before proceeding with the dark matter phenomenology, we study first constraints on the model from Higgs measurements as well as oblique parameters. The mixing angle $\theta$ between the two scalars $\rho_s$ and $\rho_h$ is constrained by the data from Higgs measurements at the LHC. Performing a universal Higgs fit [11] to the data of ATLAS and CMS collaborations, one



JHEP04(2017)034

has $\cos\theta > 0.865$ at the 95% confidence level (CL) [9, 10], which is slightly stronger than the result of global $\chi^2$ fit preformed in ref. [41].

A heavy $Z'$ with SM $Z$ couplings to fermions was searched at the LHC in the dilepton channel, which is excluded at the 95% CL for $M_{Z'} < 2.9$ TeV [12] and for $M_{Z'} < 2.79$ TeV [13]. Considering the perturbativity and RG running constraints on the gauge coupling $g_{\rm B+L}$ (see the discussions below), the lower limit on $M_{Z'}$ might imply a lower bound on the $v_s$. Phenomenological constraints also require the $Z - Z'$ mixing angle to be less than $2 \times 10^{-3}$ [14]. In our model $Z'$ mixes with $Z$ only through loop effect. This constraint can easily be satisfied, and we refer the reader to ref. [15] for the calculation of the $Z - Z'$ mixing angle in detail.

The $\beta$-function of $g_{\rm B+L}$ can be written as

$$16\pi^2\beta_{g_{\rm B+L}} = \frac{212}{3} g^3_{\rm B+L} \,, \tag{3.1}$$

which is very different from the $\beta$-function of $g_{\rm B-L}$: $16\pi^2\beta_{g_{\rm B-L}} = 12 g^3_{\rm B-L}$. Thus one may distinguish $\mathrm{U}(1)_{\rm B+L}$ from $\mathrm{U}(1)_{\rm B-L}$ by studying the running behavior of the gauge coupling. It should be mentioned that the $\beta$-function can be modified by changing the representation of extra fermions, see for instance [16, 17]. There is also constraint on $g_{\rm B+L}$ from perturbativity. A naive assumption of $g_{\rm B+L} < 1$ at the $\mu = M_{\rm Plank}$ results in $g_{\rm B+L}|_{\mu=2.9{\rm TeV}} < 0.174$. With a looser constraint on the value of $g_{\rm B+L}$ at the Planck scale $M_{\rm pl}$, $g_{\rm B+L}$ is allowed to take a larger value at the TeV scale.

We consider further the constraint from oblique observables [18, 19], which are defined in terms of contributions to the vacuum polarizations of the SM gauge bosons. One can derive the following formulae of $S$ and $T$ using gauge boson self energies $\Pi_{11}(q^2)$, $\Pi_{33}(q^2)$ and $\Pi_{3Q}(q^2)$ as given in ref. [18],

$$S = 16\pi \frac{d}{dq}\left[\Pi_{33}(q^2) - \Pi_{3Q}(q^2)\right]\Big|_{q^2=0} \,, \qquad T = \frac{4\pi}{c_w^2 s_w^2 M_Z^2}\left[\Pi_{11}(0) - \Pi_{33}(0)\right]. \tag{3.2}$$

In our model there are two separate contributions to the oblique parameters: the scalar sector and the new fermions. The dependence of $S$ and $T$ parameters on the new scalars can be approximately written as [20]

$$\Delta S = \sum_{\kappa=1}^{2} \frac{V_{1\kappa}^2}{24\pi}\left\{\log R_{\kappa h} + \hat{G}(M_\kappa^2, M_Z^2) - \hat{G}(m_h^2, M_Z^2)\right\}, \tag{3.3}$$

$$\Delta T = \sum_{\kappa=1}^{2} \frac{3V_{1\kappa}^2}{16\pi s_W^2 M_W^2}\left\{M_Z^2\left[\log\frac{R_{Z\kappa}}{1-R_{Z\kappa}} - \log\frac{R_{Zh}}{1-R_{Zh}}\right] - M_W^2\left[\log\frac{R_{W\kappa}}{1-R_{W\kappa}} - \log\frac{R_{Wh}}{1-R_{Wh}}\right]\right\}, \tag{3.4}$$

where $V$ is the mixing matrix of the CP-even scalar mass matrix, $c_W = \cos\theta_W$ with $\theta_W$ the weak mixing angle, $R_{\zeta\xi} \equiv M_\zeta^2/M_\xi^2$ and the expression of $\hat{G}(M_\zeta^2,\ M_\xi^2)$ is given in [21]. The contribution of vector like fermions to the oblique parameters are a little bit complicated. If we work in the basis wherein the charged heavy fermions are in their mass eigenstates,



JHEP04(2017)034

the left-handed and right-handed mixing matrices diagonalizing the charged fermion mass matrix are diagonal, then the expressions can be simplified to [22]

$$\begin{aligned}\pi\Delta S = & \frac{1}{3} - b_2\left(M_{E_1}, M_{E_1}, 0\right) - b_2\left(M_{E_2}, M_{E_2}, 0\right) \\ & + \sum_{j,k=1}^{4}\left(\left|\mathcal{U}_{3j}\right|^2\left|\mathcal{U}_{3k}\right|^2 + \left|\mathcal{U}_{4j}\right|^2\left|\mathcal{U}_{4k}\right|^2\right) b_2\left(M_{N_j}, M_{N_k}, 0\right) \\ & + \sum_{j,k=1}^{4}\mathrm{Re}\left(\mathcal{U}_{3j}\mathcal{U}_{3k}^*\mathcal{U}_{4j}\mathcal{U}_{4k}^*\right) f_3\left(M_{N_j}, M_{N_k}\right). \end{aligned} \tag{3.5}$$

$$\begin{aligned}4\pi s_w^2 c_w^2 M_z^2 \Delta T = & \sum_{j=1}^{2} M_{E_j}^2 b_1(M_{E_j}, M_{E_j}, 0) \\ & - 2\sum_{j=1}^{4}\left|\mathcal{U}_{3j}\right|^2 b_3\left(M_{N_j}, M_{E_1}, 0\right) - 2\sum_{j=1}^{4}\left|\mathcal{U}_{4j}\right|^2 b_3\left(M_{N_j}, M_{E_2}, 0\right) \\ & + \sum_{j,k=1}^{4}\left(\left|\mathcal{U}_{3j}\right|^2\left|\mathcal{U}_{3k}\right|^2 + \left|\mathcal{U}_{4j}\right|^2\left|\mathcal{U}_{4k}\right|^2\right) b_3\left(M_{N_j}, M_{N_k}, 0\right) \\ & - \sum_{j,k=1}^{4}\mathrm{Re}\left(\mathcal{U}_{3j}\mathcal{U}_{3k}^*\mathcal{U}_{4j}\mathcal{U}_{4k}^*\right) M_{N_j} M_{N_k} b_0\left(M_{N_j}, M_{N_k}, 0\right). \end{aligned} \tag{3.6}$$

The expressions of $b_a(x, y, z)$ can be found in ref. [22].

The constraint from oblique observables on interactions of new vector-like fermions was studied in many references [22, 29, 30]. Two extreme scenarios are: (1) No Yukawa interaction between new fermions and the SM Higgs exists, which has $\Delta S \sim \Delta T \sim 0$; (2) Only Yukawa interactions between vector-like(VL) fermions and the SM Higgs exist and the mass splitting between the members of the doublet goes to zero, which has $\Delta S \approx 0.11$ and $\Delta T = 0$ [22], that is already excluded at the 95% CL. Actually $\Delta T$ grows proportional to $\Delta m^2$, and corrections to $\Delta S$ are proportional to $\log(\Delta m^2)$, where $\Delta m^2$ is the squared mass difference of neutral and charged components in new doublet. So that there are constraints on the mass splittings of components in new fermion doublets from oblique observables, where the upper bound of mass splittings can not be certain concrete value in our model since we have multi-doublets. We show numerically in figure 1 corrections to oblique observables in the $S-T$ plane, where we set $\cos\theta > 0.865$, taken from the universal fit to the data of Higgs measurements at the LHC, and set the largest mass splitting between the heavier neutral(charged) fermions and the dark matter to be 200 GeV. The dashed and solid red curves correspond respectively to the contours at the 68% and 95% CL, which comes from the recent electroweak fit to the oblique parameters performed by the Gfitter group [28]. Obviously in a large parameter space of our model, the constraint of oblique observables can be satisfied.

Constraints from lepton colliders on the $Z'$ come from the measurement of $e^+e^- \to \bar{f}f$ above the Z-pole at the LEP-II. Lower bound on $M_{Z'}/g'$ from LEP-II was analyzed in ref. [53] for $\mathrm{U(1)_{B-xL}}$ model, where $x$ takes any value that ranges from $-3$ to $+3$. Mapping



JHEP04(2017)034

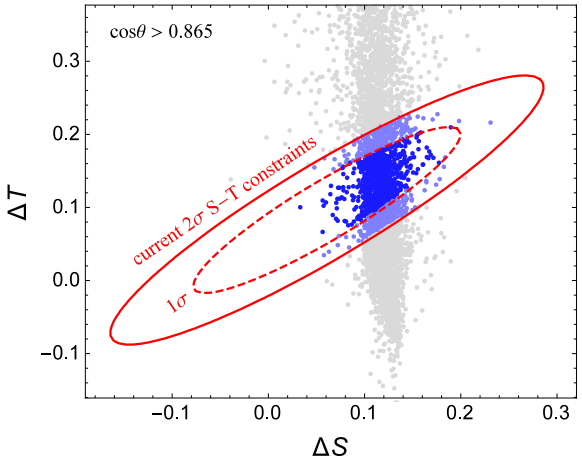


**Figure 1**. Scattering plot in the $S$-$T$ plane by setting the largest mass splitting between the heavier neutral(charged) fermions and the DM candidate to be 200 GeV, the dashed and solid contour is the allowed parameter space at the 68% and 95% C.L. respectively, given by the Gfitter group.

their results to our $\mathbf{B}+\mathbf{L}$ model, one has $M_{Z'}/g_{\mathrm{B+L}} > 6$ TeV. Compared with the current LHC constraint on the $Z'$, it puts an upper bound on the $g_{\mathrm{B+L}}$, which is about 0.48. Once $g_{\mathrm{B+L}}$ is smaller than 0.48, the LHC constraint on the $Z'$ will be stronger than that of LEP-II.

## 4 Dark matter

The fact that about 26.8% of the Universe is made of dark matter has been established. The weakly interacting massive particle (WIMP) is a promising dark matter candidate, since it can naturally get the observed relic density for a WIMP with mass around 100 GeV and interaction strength with SM particles similar to that of the weak nuclear force. In this section we take $\zeta$ as the WIMP and study its implications in relic abundance and direct detections.[1] Due to its special charge, $\zeta$ is automatically stabilized by the $\mathbf{B}+\mathbf{L}$, whose interactions are given in eq. (2.8). The phenomenology of $\zeta$ is a little similar to that of the dark matter with the $\mathbf{B}-\mathbf{L}$ symmetry, which was well-studied in many references [31–40]. Briefly speaking the thermal dark matter is in the thermal equilibrium at the early Universe and freezes out as the temperature drops down. The Boltzmann equation, governing the evolution of the dark matter density $n$, can be written as [44]

$$\dot{n} + 3Hn = -\langle\sigma v\rangle \left(n^2 - n_{\mathrm{EQ}}^2\right), \tag{4.1}$$

where $H$ is the Hubble constant, $\langle\sigma v\rangle$ is the thermal average of reduced annihilation cross sections.

One can approximate $\langle\sigma v\rangle$ with the non-relativistic expansion: $\langle\sigma v\rangle = a + b\langle v^2\rangle$ and the contributions from various channels are

$$\langle\sigma v\rangle_{s_a s_b} = \frac{1}{1+\delta}\frac{\lambda^{1/2}(4,\boldsymbol{\lambda}_a,\boldsymbol{\lambda}_b)}{256\pi m_\zeta^4}\left|\frac{\widehat{\mathcal{C}}_1 C_{sab}}{4-\boldsymbol{\lambda}_s}+\frac{\widehat{\mathcal{C}}_2 C_{hab}}{4-\boldsymbol{\lambda}_h}\right|^2\langle v^2\rangle \tag{4.2}$$

[1]For the indirect detection signal of this kind of dark matter, we refer the reader to ref. [45] for detail.



JHEP04(2017)034

$$\langle\sigma v\rangle_{VV} = \frac{1}{128\pi m_\zeta^4}\sqrt{1-\boldsymbol{\lambda}_V}\left(3-\frac{4}{\boldsymbol{\lambda}_V}+\frac{4}{\boldsymbol{\lambda}_V^2}\right)\left|\frac{\widehat{\mathcal{C}}_1 C_{sVV}}{4-\boldsymbol{\lambda}_s}+\frac{\widehat{\mathcal{C}}_2 C_{hVV}}{4-\boldsymbol{\lambda}_h}\right|^2\langle v^2\rangle, \tag{4.3}$$

$$\begin{aligned}\langle\sigma v\rangle_{WW} = {}& \frac{1}{64\pi m_\zeta^4}\sqrt{1-\boldsymbol{\lambda}_W}\left(3-\frac{4}{\boldsymbol{\lambda}_W}+\frac{4}{\boldsymbol{\lambda}_W^2}\right)\left|\frac{\widehat{\mathcal{C}}_1 C_{sWW}}{4-\boldsymbol{\lambda}_s}+\frac{\widehat{\mathcal{C}}_2 C_{hWW}}{4-\boldsymbol{\lambda}_h}\right|^2\langle v^2\rangle \\ & + \frac{g^2 c_W^2}{24\pi m_\zeta^2}\sqrt{1-\boldsymbol{\lambda}_W}(1-\boldsymbol{\lambda}_W)\left(3+\frac{20}{\boldsymbol{\lambda}_W}+\frac{4}{\boldsymbol{\lambda}_W^2}\right)\left|\frac{\mathcal{C}_4}{4-\boldsymbol{\lambda}_Z}\right|^2\langle v^2\rangle,\end{aligned} \tag{4.4}$$

$$\begin{aligned}\langle\sigma v\rangle_{f\bar{f}} = {}& \frac{n_C^f}{8\pi m_\zeta^2}(1-\boldsymbol{\lambda}_f)^{3/2}\left|\frac{\widehat{\mathcal{C}}_1 C_{sf\bar{f}}}{4-\boldsymbol{\lambda}_s}+\frac{\widehat{\mathcal{C}}_2 C_{hf\bar{f}}}{4-\boldsymbol{\lambda}_h}\right|^2\langle v^2\rangle \\ & + \sum_X^{Z,Z'}\frac{n_C^f}{12\pi m_\zeta^2}\sqrt{1-\boldsymbol{\lambda}_f}\,(\boldsymbol{\lambda}_f+2)\left|\frac{\mathcal{C}_V g_X^V}{4-\boldsymbol{\lambda}_V}\right|^2\langle v^2\rangle + \frac{n_C^f \mathcal{C}_4^2 g_Z^{A2}\varrho_Z^f\sqrt{1-\boldsymbol{\lambda}_f}}{2\pi m_Z^2} \\ & + \frac{23\boldsymbol{\lambda}_f^2-192\varrho_Z^f\boldsymbol{\lambda}_Z^{-1}+8(30\varrho_Z^{f2}+12\varrho_Z^f+1)-4\boldsymbol{\lambda}_f(30\varrho_Z^f+7)}{48\pi m_\zeta^2\sqrt{1-\boldsymbol{\lambda}_f}}\frac{n_C^f\mathcal{C}_4^2 g_Z^{A2}}{\left|4-\boldsymbol{\lambda}_Z\right|^2}\langle v^2\rangle \\ & + n_C^f\frac{\sqrt{1-\boldsymbol{\lambda}_f}(2+\boldsymbol{\lambda}_f)}{6\pi m_\zeta^2}\mathrm{Re}\left[\frac{\mathcal{C}_3\mathcal{C}_4 g_Z^V g_{Z'}^V}{(4-\boldsymbol{\lambda}_{Z'})(4-\boldsymbol{\lambda}_Z)^*}\right]\langle v^2\rangle,\end{aligned} \tag{4.5}$$

$$\langle\sigma v\rangle_{Vs} = \mathcal{C}_{V\zeta\zeta}^2\mathcal{C}_{sVV}^2\frac{\lambda^{3/2}(4,\boldsymbol{\lambda}_V,\boldsymbol{\lambda}_s)}{1024\pi m_\zeta^4\boldsymbol{\lambda}_V^3}+\mathcal{O}(\langle v^2\rangle) \tag{4.6}$$

where $\boldsymbol{\lambda}_X = m_X^2/m_\zeta^2$, $\varrho_V^f = m_f^2/m_V^2$, $V = Z,\ Z'$; $\delta_{ab} = 1$ (for $a = b$) and 0 (for $a \neq b$); the trilinear couplings $C_{s_i s_j s_k}$ are given in table. 2; $g_Z^V = \frac{e}{2}(-\frac{s_W}{c_W}Q_f + \frac{I_f^3 - s_W^2 Q_f}{s_W c_W})$, $g_Z^A = \frac{e}{2}(-\frac{s_W}{c_W}Q_f - \frac{I_f^3 - s_W^2 Q_f}{s_W c_W})$ with $Q_f$, $s_W$, $I_f^3$ being the electric charge, weak mixing angle and the third component of the iso-spin respectively. If the mediator is close to its mass shell, one needs to do the replacement $4-\lambda_X \to 4-\lambda_X + i\Gamma_X m_X/m_\zeta^2$. Notice that eq. (4.6) is simplified by neglecting terms proportional to $\langle v^2\rangle$, which is lengthy, but we keep them in numerical calculations.

Given these results, the final relic density can be written as

$$\Omega h^2 \approx \frac{1.07\times 10^9\ \mathrm{GeV}^{-1}}{M_{pl}}\frac{x_F}{\sqrt{g_\star}}\frac{1}{a+3b/x_F}, \tag{4.7}$$

where $M_{pl}$ is the planck mass, $x_F \approx m_\zeta/T_F$, with $T_F$ the freeze-out temperature, $g_\star$ is the degree of the freedom at $T_F$. We show in figure 2 the scattering plot of $\Omega h^2$ as the function of the dark matter mass by fixing $m_s = 750$ GeV and $M_{Z'} = 3$ TeV. For the sake of clarity, we set the widths $\Gamma_s = 1$ GeV and $\Gamma_{Z'} = 10$ GeV. We work in the basis where the mass matrix of heavy charged fermions is diagonal, while the masses of heavy neutral fermions (including the dark matter candidate $\zeta$) and the mixing angles among them are random parameters. The VEV $v_s$ also varies from 1.5 TeV to 3 TeV, which renders that the gauge coupling $g_{B+L}$ goes from 0.17 to 0.33 via equation (2.4). Note that $v_s$ can not be too small, or some of the Yukawa couplings $y_i$ are pushed to be unacceptably large by $v_s^{-1}$, cf. table 3. In this plot the constraints of oblique parameters are also taken into consideration, at the



JHEP04(2017)034

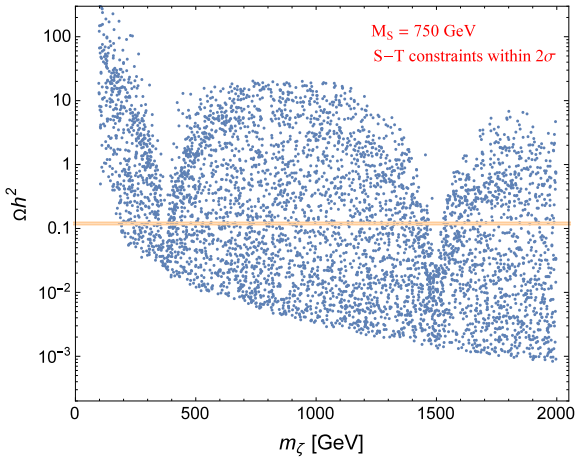


**Figure 2**. Scattering plot for the relic density of dark matter $\Omega h^2$ versus its mass $m_\zeta$, with $m_s = 750\,\text{GeV}$. The $S$, $T$ constraints are applied at the 95% C.L.. The horizontal orange line is the current relic density $0.1197 \pm 0.0022$.

95% C.L.. The horizontal line is the observed relic density value of $0.1197 \pm 0.0022$. The first and second valleys around 375 GeV and 1.5 TeV come respectively from the resonance enhancement of $s$ and $Z'$ to the annihilation cross section.

The particle dark matter can be tested directly via scattering on target nuclei. In our model the dark matter has both spin-dependent (SI) and spin-independent (SD) scattering with nuclei mediated by scalars $(h, s)$ and $Z$ respectively. The effective Lagrangian for the scalar interactions can be written as

$$\mathcal{L}_{\text{SI}} = \left( \frac{\widehat{\mathcal{C}}_2 c_\theta}{m_h^2} - \frac{\widehat{\mathcal{C}}_1 s_\theta}{m_s^2} \right) \frac{1}{v_h} \bar{\zeta}\zeta\bar{q} m_q q \,. \tag{4.8}$$

It leads to the following expression for the cross section of a Majorana dark matter particle at the zero-momentum transfer,

$$\sigma_{\text{SI}} = \frac{4\mu^2}{\pi v_h^2} \left( \frac{\widehat{\mathcal{C}}_2 c_\theta}{m_h^2} - \frac{\widehat{\mathcal{C}}_1 s_\theta}{m_s^2} \right)^2 \left[ Z f_p + (A - Z) f_n \right]^2 \tag{4.9}$$

where $\mu$ is the reduced mass of WIMP-nucleus system, $f_{p,n} = m_{p,n}(2/9 + 7/9 \sum_{q=u,d,s} f_{T_q}^{p,n})$. One has $f_{T_u}^p = 0.020 \pm 0.004$, $f_{T_d}^p = 0.026 \pm 0.005$, $f_{T_u}^n = 0.014 \pm 0.003$, $f_{T_d}^n = 0.036 \pm 0.008$, and $f_s^{p,n} = 0.118 \pm 0.062$ [23].

We show in the left panel of figure 3 the scattering plot of the SI cross section as the function of $m_\zeta$ for the general case, where inputs are given as $m_s = 750$ GeV, $m_{Z'} = 3$ TeV, $|\mathcal{U}_{31}^2 - \mathcal{U}_{41}^2| < 0.1$ and $|\sin\theta_{ij}| < 0.8$, with $\theta_{ij}$ the mixing angles in $\mathcal{U}$. For each point in the plot one has $\Omega h^2 \in (0.1197 - 3 \times 0.0022,\ 0.1197 + 3 \times 0.0022)$, while the oblique parameters $S$ and $T$ lie in the $2\sigma$ contour as shown in figure 1. The magenta, green and blue points correspond to cases where $f\bar{f}$, $VV$ and $Vs(h)$ final states dominate the annihilation of $\zeta$ respectively. The red solid and the purple dashed lines are the exclusion limits of the LUX 2016 [42] and PandaX-II [43] respectively. We show in the right panel of figure 3 the $\sigma^{\text{SI}}$ as



JHEP04(2017)034

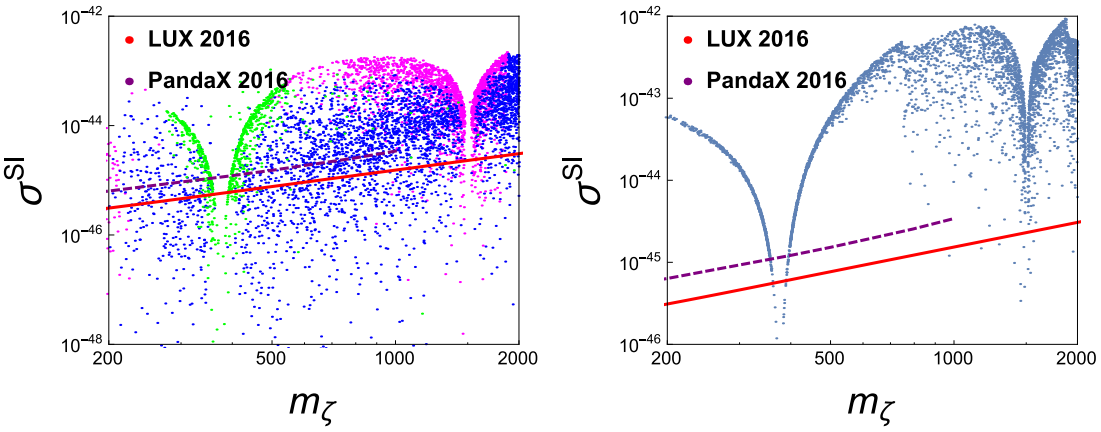


**Figure 3**. $\sigma^{\rm SI}$ as the function of $m_\zeta$ for the general (left panel) and simplified (right panel) cases respectively, where the simplified case means $\psi_{L,R}$ are decoupled. All points in the plots give the relic density within the $3\sigma$ deviation from the observed central value. Constraints of oblique observables within $2\sigma$ are also taken into consideration.

the function of $m_\zeta$ for a simplified case, where $\psi_{L,R}$ are decoupled from the singlets $\chi_{L,R}$. We set $m_s = 750$ GeV and $m_{Z'} = 3$ TeV when making the plot, while $m_\zeta$ and $v_s$ are free parameters. All the points in the plot give a relic density within the $3\sigma$ deviation from the observed central value of 0.1197. One can conclude from the plot that this scenario is available only for $m_\zeta \approx m_s/2$, where the annihilation cross section is resonantly enhanced, and for $m_\zeta > m_s$ where new annihilation channel is open.

The effective Lagrangian for the axial-vector interaction, which is relevant to the SD scattering of DM from nuclei, can be written as

$$\mathcal{L}_{\rm SD} = \frac{\mathcal{C}_4 g_Z^A}{M_Z^2} \bar{\zeta}\gamma_\mu\gamma_5\zeta\bar{q}\gamma_\mu\gamma_5 q, \tag{4.10}$$

There are also effective interaction of the form: $\bar{\zeta}\gamma_\mu\gamma_5\zeta\bar{q}\gamma^\mu q$. It turns out that the corresponding matrix elements are suppressed by the tiny dark matter velocity, whose contribution to the direct detection is thus negligible considering $v_{\rm DM} \sim 10^{-3}$. The expression for the SD cross section for the Majorana particle takes the form

$$\sigma^{\rm SD} = \frac{16\mu^2}{\pi}\left(\frac{\mathcal{C}_4}{M_Z^2}\right)^2 \left[\sum_{q=u,d,s} (g_Z^A)_q \lambda_q\right]^2 J_N(J_N+1). \tag{4.11}$$

The value of $\lambda_q$ depends on the nucleus. It reduces to $\Delta_q^p(\Delta_q^n)$, for scattering off free proton(neutron). $J_N$ is the total angular momentum quantum number of the nucleus, which equals to 1/2 for free nucleons.

In figure 4 we show constraint on $\mathcal{C}_4$ from the latest spin-dependent WIMP-neutrino cross section limits given by the LUX and PandaX-II experiments [24, 25]. Since the majority of nuclear spins are carried by the unpaired neutron, the neutron sensitivity is much higher than the proton case. The solid line is the constraint of LUX, while the



JHEP04(2017)034

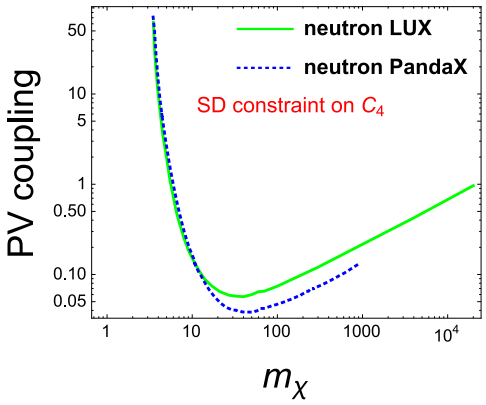


**Figure 4**. Constraints on the coupling $\mathcal{C}_4$ from the LUX result of spin-dependent DM-nucleon cross section.

dotted line is the constraint given by PandaX-II. The smallest WIMP-neutron cross section is $\sigma_n = 4.3 \times 10^{-41}$ cm$^2$ at $m_\zeta = 45$ GeV from the PandaX-II [25]. It corresponds to an upper limit of 0.037 on the coupling $\mathcal{C}_4$, which, when translated to constraint on mixing matrix elements, gives $|\mathcal{U}_{41}^2 - \mathcal{U}_{31}^2| < 0.19$ at the 90% confidence level. It is a quite loose constraint, while future measurement of $\sigma^{\rm SD}$ from LUX-ZEPLIN may improve the current limit by a factor 15 [26].

## 5 Collider signatures

The DM could be pair produced at high energy colliders, in association with SM particles in the final states. As for many other DM scenarios, the most stringent collider constraints on our model come from the mono-jet searches, i.e. a high $p_T$ jet plus large missing $E_T$ from the DM pairs. The most recent ATLAS 13 TeV data set upper bounds of 553 fb on the beyond SM contribution to monojet signals with the leading jet $p_T > 250$ GeV and $|\eta| < 2.4$ [46], and we use this limit to constrain the effective $C_i$ couplings in our model. Indicated by the $C_i$ couplings in eq. (8), the DM in our model can be pair produced through the scalars $h$, $S$, or the vector bosons $Z$ and $Z'$. The heavy scalar $S$ couples to the SM quarks (and leptons) via its mixing to the SM Higgs $h$, thus its production is also dominated by the gluon fusion channel, yet further suppressed by the scalar mixing $\sin\theta$. However, when the DM mass lies in the range $M_h/2 < m_\zeta < M_S/2$, the heavy scalar might dominate the scalar channel, which however depends largely on the scalar mixing angle $\sin\theta$. The monojet constraints in the scalar, $Z$ and $Z'$ channels are depicted in figure 5. For simplicity we have set $C_1 = C_2$ and $\cos\theta = 0.865$ in the scalar channel, thus we have a kink around $m_\zeta \simeq M_S/2$ beyond which the constraint is rather loose. In the $Z$ channel, when DM is light, say $m_\zeta \sim 100$ GeV, the coupling $C_4$ is constrained at the order of one. However, when DM becomes heavier, the phase space shrinks rapidly and the the constraint goes weaker very quickly. For the $Z'$ channel, it is a bit different. As for a below TeV DM, $M_{Z'} > 2m_\zeta$, and thus as long as $m_\zeta/M_{Z'} \ll 1$ the constraints on $C_3$



JHEP04(2017)034

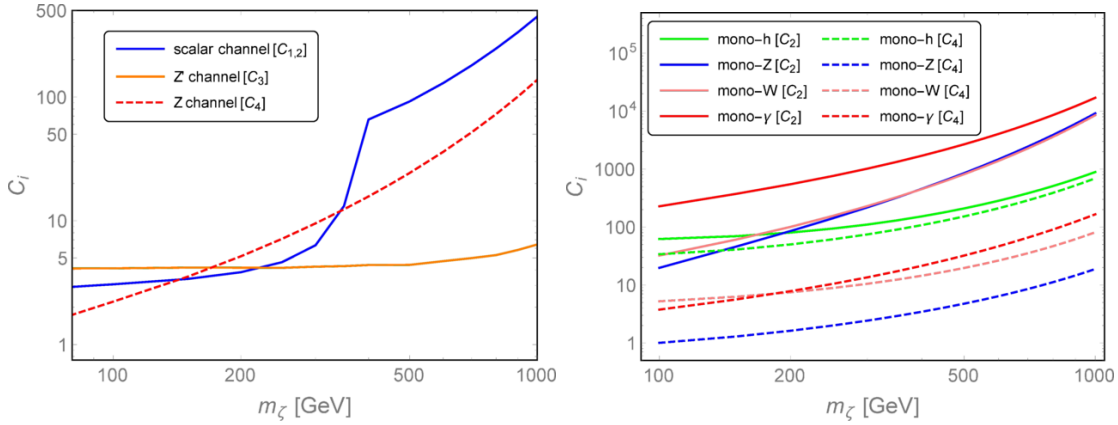


**Figure 5**. *Left panel*: constraints on the effective couplings $C_i$ of DM in the monojet channel from 13 TeV ATLAS data [46]. *Right panel*: constraints on the effective DM couplings $C_i$ in the mono-Higgs, mono-$W/Z$ and mono-photon channels. For simplicity in both the panels we have set $C_1 = C_2$ and the scalar mixing $\cos\theta = 0.865$. See text for more details.

does not change too much. However, on the other hand, suppressed by the large $Z'$ mass limit [47], the coupling $C_3$ could only be constrained to be at the order of 5, which does not help too much on constraining the parameter space. With more data accumulating at LHC and the projected future higher energy colliders, it is promising that our model could be constrained by future collider data, which is then complementary to the direct detection experiments at much lower energies.

In addition to the monojet channel, we can have also the pair production of DM with an SM EW boson, i.e. the mono-Higgs, mono-$W$, mono-$Z$ and mono-photon channels. All these searches have been performed at the LHC Run II [48–52]. As a rough re-interpretation of these DM limits at colliders in terms of our present model, we apply the basic cuts in these analysis, and use the number of background events and the background uncertainties to estimate the constraints on beyond SM contribution. For simplicity we switch off the mediators $S$ and $Z'$ and consider only the constraints on the couplings to the SM Higgs and $Z$ bosons, i.e. the effective couplings $C_{2,4}$. It is found that the constraints in these mono-*boson* searches are in general much weaker than the mono-jet channel. Benefiting from the large $Z$ production rate, only the mono-$Z$ channel could constrain the coupling $C_4$ of DM to $Z$ boson at the level of 1 to 10, which is comparable to the monojet searches in some region of the parameter space of interest.

## 6 Conclusion

In this paper, we extended the SM with a local $\mathbf{B} + \mathbf{L}$ symmetry and shown that the lightest extra fermion, which was introduced to cancel anomalies, can serve as a cold dark matter candidate. Constraints on the model from Higgs measurements and electroweak precision measurements were studied. Further applying these constraints to the dark matter, we searched for available parameter space that can give the correct relic density and satisfy the constraints of spin-independent and spin-dependent direct detections in the meanwhile.



JHEP04(2017)034

The model possesses adequate parameter space that satisfies all constraints. This model is complementary to the $\mathbf{B}-\mathbf{L}$ extension of the SM, and deserves further study on either the model itself or the collider phenomenology. It will be also interesting to investigate the baryon asymmetry of the Universe in this model, which, although interesting but beyond the reach of this paper, will be shown in the future study.

## Acknowledgments

This work of W.C. and H.G. were supported in part by DOE Grant DE-SC0011095. H.G. was also supported by the China Scholarship Council. Y.Z. would like to thank the IISN and Belgian Science Policy (IAP VII/37) for support.



## References

[1] Planck collaboration, P.A.R. Ade et al., *Planck 2015 results. XIII. Cosmological parameters*, *Astron. Astrophys.* **594** (2016) A13 [arXiv:1502.01589] [INSPIRE].

[2] P. Fileviez Perez and M.B. Wise, *Baryon and lepton number as local gauge symmetries*, *Phys. Rev.* **D 82** (2010) 011901 [*Erratum ibid.* **D 82** (2010) 079901] [arXiv:1002.1754] [INSPIRE].

[3] P. Fileviez Perez and M.B. Wise, *Breaking Local Baryon and Lepton Number at the TeV Scale*, *JHEP* **08** (2011) 068 [arXiv:1106.0343] [INSPIRE].

[4] M. Duerr, P. Fileviez Perez and M.B. Wise, *Gauge Theory for Baryon and Lepton Numbers with Leptoquarks*, *Phys. Rev. Lett.* **110** (2013) 231801 [arXiv:1304.0576] [INSPIRE].

[5] J.M. Arnold, P. Fileviez Pérez, B. Fornal and S. Spinner, *B and L at the supersymmetry scale, dark matter and R-parity violation*, *Phys. Rev.* **D 88** (2013) 115009 [arXiv:1310.7052] [INSPIRE].

[6] B. Fornal, *Minimal supersymmetric standard model with gauged baryon and lepton numbers*, *Int. J. Mod. Phys.* **A 30** (2015) 1530027 [arXiv:1503.09009] [INSPIRE].

[7] R.N. Mohapatra and R.E. Marshak, *Local B-L Symmetry of Electroweak Interactions, Majorana Neutrinos and Neutron Oscillations*, *Phys. Rev. Lett.* **44** (1980) 1316 [*Erratum ibid.* **44** (1980) 1643] [INSPIRE].

[8] W. Chao, *Pure Leptonic Gauge Symmetry, Neutrino Masses and Dark Matter*, *Phys. Lett.* **B 695** (2011) 157 [arXiv:1005.1024] [INSPIRE].

[9] W. Chao, *Symmetries behind the 750 GeV diphoton excess*, *Phys. Rev.* **D 93** (2016) 115013 [arXiv:1512.06297] [INSPIRE].

[10] W. Chao, *Hiding Scalar Higgs Portal Dark Matter*, arXiv:1601.06714 [INSPIRE].

[11] P.P. Giardino, K. Kannike, I. Masina, M. Raidal and A. Strumia, *The universal Higgs fit*, *JHEP* **05** (2014) 046 [arXiv:1303.3570] [INSPIRE].



JHEP04(2017)034

[12] ATLAS collaboration, *Search for high-mass dilepton resonances in pp collisions at $\sqrt{s} = 8$ TeV with the ATLAS detector*, *Phys. Rev.* **D 90** (2014) 052005 [arXiv:1405.4123] [INSPIRE].

[13] CMS collaboration, *Search for physics beyond the standard model in dilepton mass spectra in proton-proton collisions at $\sqrt{s} = 8$ TeV*, *JHEP* **04** (2015) 025 [arXiv:1412.6302] [INSPIRE].

[14] J. Erler, P. Langacker, S. Munir and E. Rojas, *Improved Constraints on Z-prime Bosons from Electroweak Precision Data*, *JHEP* **08** (2009) 017 [arXiv:0906.2435] [INSPIRE].

[15] W. Chao and M.J. Ramsey-Musolf, *Hidden from view: Neutrino masses, dark matter and TeV-scale leptogenesis in a neutrinophilic two-Higgs-doublet model*, *Phys. Rev.* **D 89** (2014) 033007 [arXiv:1212.5709] [INSPIRE].

[16] W. Chao, M. Gonderinger and M.J. Ramsey-Musolf, *Higgs Vacuum Stability, Neutrino Mass and Dark Matter*, *Phys. Rev.* **D 86** (2012) 113017 [arXiv:1210.0491] [INSPIRE].

[17] R.N. Mohapatra and Y. Zhang, *TeV Scale Universal Seesaw, Vacuum Stability and Heavy Higgs*, *JHEP* **06** (2014) 072 [arXiv:1401.6701] [INSPIRE].

[18] M.E. Peskin and T. Takeuchi, *Estimation of oblique electroweak corrections*, *Phys. Rev.* **D 46** (1992) 381 [INSPIRE].

[19] M.E. Peskin and T. Takeuchi, *A new constraint on a strongly interacting Higgs sector*, *Phys. Rev. Lett.* **65** (1990) 964 [INSPIRE].

[20] W. Grimus, L. Lavoura, O.M. Ogreid and P. Osland, *The oblique parameters in multi-Higgs-doublet models*, *Nucl. Phys.* **B 801** (2008) 81 [arXiv:0802.4353] [INSPIRE].

[21] W. Chao, M.J. Ramsey-Musolf and J.-H. Yu, *Indirect Detection Imprint of a CP-violating Dark Sector*, *Phys. Rev.* **D 93** (2016) 095025 [arXiv:1602.05192] [INSPIRE].

[22] A. Joglekar, P. Schwaller and C.E.M. Wagner, *Dark Matter and Enhanced Higgs to Di-photon Rate from Vector-like Leptons*, *JHEP* **12** (2012) 064 [arXiv:1207.4235] [INSPIRE].

[23] J.R. Ellis, A. Ferstl and K.A. Olive, *Reevaluation of the elastic scattering of supersymmetric dark matter*, *Phys. Lett.* **B 481** (2000) 304 [hep-ph/0001005] [INSPIRE].

[24] LUX collaboration, D.S. Akerib et al., *Results on the Spin-Dependent Scattering of Weakly Interacting Massive Particles on Nucleons from the Run 3 Data of the LUX Experiment*, *Phys. Rev. Lett.* **116** (2016) 161302 [arXiv:1602.03489] [INSPIRE].

[25] PandaX-II collaboration, C. Fu et al., *Spin-Dependent Weakly-Interacting-Massive-Particle-Nucleon Cross section Limits from First Data of PandaX-II Experiment*, *Phys. Rev. Lett.* **118** (2017) 071301 [arXiv:1611.06553] [INSPIRE].

[26] LZ collaboration, D.S. Akerib et al., *LUX-ZEPLIN (LZ) Conceptual Design Report*, arXiv:1509.02910 [INSPIRE].

[27] M. Fairbairn and P. Grothaus, *Baryogenesis and Dark Matter with Vector-like Fermions*, *JHEP* **10** (2013) 176 [arXiv:1307.8011] [INSPIRE].

[28] M. Baak et al., *The Electroweak Fit of the Standard Model after the Discovery of a New Boson at the LHC*, *Eur. Phys. J.* **C 72** (2012) 2205 [arXiv:1209.2716] [INSPIRE].

[29] F. del Aguila, J. de Blas and M. Pérez-Victoria, *Effects of new leptons in Electroweak Precision Data*, *Phys. Rev.* **D 78** (2008) 013010 [arXiv:0803.4008] [INSPIRE].

[30] G. Cynolter and E. Lendvai, *Electroweak Precision Constraints on Vector-like Fermions*, *Eur. Phys. J.* **C 58** (2008) 463 [arXiv:0804.4080] [INSPIRE].

JHEP04(2017)034

[31] L. Basso, B. O'Leary, W. Porod and F. Staub, *Dark matter scenarios in the minimal SUSY B-L model*, *JHEP* **09** (2012) 054 [arXiv:1207.0507] [INSPIRE].

[32] J. Guo, Z. Kang, P. Ko and Y. Orikasa, *Accidental dark matter: Case in the scale invariant local B-L model*, *Phys. Rev.* **D 91** (2015) 115017 [arXiv:1502.00508] [INSPIRE].

[33] S. Baek, H. Okada and T. Toma, *Two loop neutrino model and dark matter particles with global B-L symmetry*, *JCAP* **06** (2014) 027 [arXiv:1312.3761] [INSPIRE].

[34] B.L. Sánchez-Vega and E.R. Schmitz, *Fermionic dark matter and neutrino masses in a B-L model*, *Phys. Rev.* **D 92** (2015) 053007 [arXiv:1505.03595] [INSPIRE].

[35] W. Rodejohann and C.E. Yaguna, *Scalar dark matter in the B-L model*, *JCAP* **12** (2015) 032 [arXiv:1509.04036] [INSPIRE].

[36] A. El-Zant, S. Khalil and A. Sil, *Warm dark matter in a B-L inverse seesaw scenario*, *Phys. Rev.* **D 91** (2015) 035030 [arXiv:1308.0836] [INSPIRE].

[37] T. Li and W. Chao, *Neutrino Masses, Dark Matter and B-L Symmetry at the LHC*, *Nucl. Phys.* **B 843** (2011) 396 [arXiv:1004.0296] [INSPIRE].

[38] N. Okada and O. Seto, *Higgs portal dark matter in the minimal gauged* $\mathrm{U}(1)_{B-L}$ *model*, *Phys. Rev.* **D 82** (2010) 023507 [arXiv:1002.2525] [INSPIRE].

[39] Z.M. Burell and N. Okada, *Supersymmetric minimal B-L model at the TeV scale with right-handed Majorana neutrino dark matter*, *Phys. Rev.* **D 85** (2012) 055011 [arXiv:1111.1789] [INSPIRE].

[40] N. Okada and S. Okada, $Z'_{BL}$ *portal dark matter and LHC Run-2 results*, *Phys. Rev.* **D 93** (2016) 075003 [arXiv:1601.07526] [INSPIRE].

[41] S. Profumo, M.J. Ramsey-Musolf, C.L. Wainwright and P. Winslow, *Singlet-catalyzed electroweak phase transitions and precision Higgs boson studies*, *Phys. Rev.* **D 91** (2015) 035018 [arXiv:1407.5342] [INSPIRE].

[42] LUX collaboration, D.S. Akerib et al., *Results from a search for dark matter in the complete LUX exposure*, *Phys. Rev. Lett.* **118** (2017) 021303 [arXiv:1608.07648] [INSPIRE].

[43] PandaX-II collaboration, A. Tan et al., *Dark Matter Results from First 98.7 Days of Data from the PandaX-II Experiment*, *Phys. Rev. Lett.* **117** (2016) 121303 [arXiv:1607.07400] [INSPIRE].

[44] G. Bertone, D. Hooper and J. Silk, *Particle dark matter: Evidence, candidates and constraints*, *Phys. Rept.* **405** (2005) 279 [hep-ph/0404175] [INSPIRE].

[45] M. Duerr, P. Fileviez Perez and J. Smirnov, *Gamma Lines from Majorana Dark Matter*, *Phys. Rev.* **D 93** (2016) 023509 [arXiv:1508.01425] [INSPIRE].

[46] ATLAS collaboration, *Search for new phenomena in final states with an energetic jet and large missing transverse momentum in pp collisions at* $\sqrt{s} = 13$ *TeV using the ATLAS detector*, *Phys. Rev.* **D 94** (2016) 032005 [arXiv:1604.07773] [INSPIRE].

[47] ATLAS collaboration, *Search for high-mass new phenomena in the dilepton final state using proton-proton collisions at* $\sqrt{s} = 13$ *TeV with the ATLAS detector*, *Phys. Lett.* **B 761** (2016) 372 [arXiv:1607.03669] [INSPIRE].

[48] ATLAS collaboration, *Search for Dark Matter in association with a Higgs boson decaying to b-quarks in pp collisions at* $\sqrt{s} = 13$ *TeV with the ATLAS detector*, ATLAS-CONF-2016-019 (2016).



JHEP04(2017)034

[49] CMS collaboration, *Search for dark matter production in association with jets, or hadronically decaying W or Z boson at* $\sqrt{s} = 13$ *TeV*, CMS-PAS-EXO-16-013 (2016).

[50] CMS collaboration, *Search for dark matter in* $\mathrm{Z} + E_{\mathrm{T}}^{\mathrm{miss}}$ *events using* 12.9 $\mathrm{fb}^{-1}$ *of 2016 data*, CMS-PAS-EXO-16-038 (2016).

[51] ATLAS collaboration, *Search for dark matter produced in association with a hadronically decaying vector boson in pp collisions at* $\sqrt{s} = 13$ *TeV with the ATLAS detector*, *Phys. Lett.* **B 763** (2016) 251 [arXiv:1608.02372] [INSPIRE].

[52] CMS collaboration, *Search for dark matter and graviton produced in association with a photon in pp collisions at* $\sqrt{s} = 13$ TeV *with an integrated luminosity of* 12.9 $\mathrm{fb}^{-1}$, CMS-PAS-EXO-16-039 (2016).

[53] M. Carena, A. Daleo, B.A. Dobrescu and T.M.P. Tait, $Z'$ *gauge bosons at the Tevatron*, *Phys. Rev.* **D 70** (2004) 093009 [hep-ph/0408098] [INSPIRE].

JHEP04(2017)034